A modified transfer matrix approach to include Zeeman spin splitting in dispersion relations for coupled quantum wells.

A Hernández-Cabrera and P Aceituno

Departamento de Física, Universidad de La Laguna, La Laguna, 38206-Tenerife, Spain, and Instituto Universitario de Estudios Avanzados (IUdEA) en Física Atómica, Molecular y Fotónica, Universidad de La Laguna, La Laguna, 38206 Tenerife, Spain

E-mail: ajhernan@ull.edu.es

Abstract. In our work, we calculate the dispersion relations for $InGaAs - InAlAs$ based double quantum wells (narrow gap structures). We have developed an improved 4×4 version of the Transfer Matrix Approach, considering contributions from external fields when tunneling through central barrier exists. The transverse electric field is necessary to reach the resonance of electronic levels in asymmetric structures. The in-plane magnetic field induces the Zeeman effect and the spin splitting of the resonant levels. We have also included abrupt barrier effects due to the nature of the interfaces between the above materials.

1. Introduction

The use of spin better than charge in electronic devices is known as spintronics. The low power consumption as well as the slightly dissipative transport are advantages of spin-based electronics that have made it a center of interest in last years. In order to make the most of its applications, the choice of material is a crucial point. Those with a narrow gap but a large Landé factor, which will have a large spin-orbit coupling, seem to be a good option, as $InGaAs - InAlAs$ structures are. To be useful in practice, electronic (or hole) states with different spins must be separated in energy. Moreover, the material must be electrically polarized [1].

In this work we analyze variations of the spin splitting in asymmetric structures, such as asymmetric coupled quantum wells (ACQW), when transverse electric and in plane magnetic fields are applied. We use an improved variant of 8×8 Kane formalism for the dispersion relations in the vicinity of the spin anticrossings together with a 4×4 modified version of the Transfer Matrix Approach . We have included contributions of the Pauli Hamiltonian and its mixing with the effective spìn-orbit interaction, and spin splitting caused by abrupt interfaces.

2. Eigenstate problem

In the parabolic approximation we can write the Schrödinger equation for ACQW in the form [2]:

$$\left(\varepsilon_p^\mu + \frac{\hat{p}_z^2}{2m_\mu} + \varepsilon_c^\mu(z) + \widehat{W}^\mu\right)\Psi^\mu(\mathbf{p},z) = E\Psi^\mu(\mathbf{p},z), \tag{1}$$

for the eigenfunctions $\Psi^{\mu}(\mathbf{p},z)$ and eigenvalues E. Here $\mu = b, w$ denotes de barrier and well regions, respectively. In the above equation ε_p^{μ} is the kinetic energy in the in-plane direction, which includes the effective mass m_{μ}. The $\varepsilon_c^{\mu}(z)$ energy is $U(z)$ in the wells, and $\Delta E_c + U(z)$ in the barriers, where $U(z) \simeq eF_{\perp}z$ for an uniform transverse electric field $F_{\perp}$, and ΔE_c is the band offset for conduction band. Band diagram for ACQW is shown in Fig. 1.

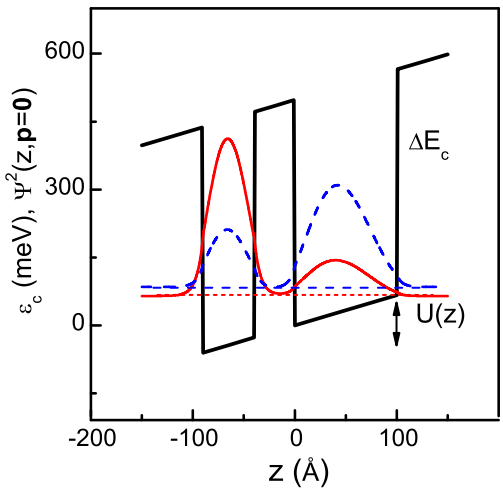

Figure 1. Conduction band diagram for asymmetric coupled quantum well. Horizontal thin lines show electron energy levels and thin curves correspond to squared wave functions close to the resonance.

The magnetic energy is described by $\widehat{W}^{\mu} = \overline{v}^{\mu}\left[\hat{\sigma} \times \mathbf{p}\right]_z + w_H^{\mu}\hat{\sigma}_y$, where $\hat{\sigma}$ is the Pauli matrix. We define the Pauli splitting energy (half of the Zeeman splitting) caused by the magnetic field as $w_H^{\mu} = (\overline{g}^{\mu}/2)\mu_B H$. Here $\overline{g}^{\mu}$ is the effective Landé factor, μ_B is the Bohr magneton, and H is the in plane magnetic field. We can take characteristic spin velocity for each layer as $\overline{v}^{\mu} = eF_{\perp}\hbar/4m_{\mu}\varepsilon_g$, with ε_g the well gap energy.

After some cumbersome algebra [3], we obtain the fundamental solutions of Eq (1):

$$\Psi^{\mu+}(\mathbf{p},z) = \left\{\left[a_{\mu+}A_i(\xi_{\mathbf{p}}^{\mu+}) + b_{\mu+}B_i(\xi_{\mathbf{p}}^{\mu+})\right] + \rho^{\mu-}(\mathbf{p})\left[a_{\mu-}A_i(\xi_{\mathbf{p}}^{\mu-}) + b_{\mu-}B_i(\xi_{\mathbf{p}}^{\mu-})\right]\right\}(1/\sqrt{2})$$
$$\Psi^{\mu-}(\mathbf{p},z) = \left\{\rho^{\mu+}(\mathbf{p})\left[a_{\mu+}A_i(\xi_{\mathbf{p}}^{\mu+}) + b_{\mu+}B_i(\xi_{\mathbf{p}}^{\mu+})\right] + \left[a_{\mu-}A_i(\xi_{\mathbf{p}}^{\mu-}) + b_{\mu-}B_i(\xi_{\mathbf{p}}^{\mu-})\right]\right\}(1/\sqrt{2}), \quad (2)$$

where $\rho^{\mu\pm}(\mathbf{p}) = (\overline{v}^{\mu}p_{\pm} + w_H^{\mu})/iw_{\mathbf{p}}^{\mu}$, with $p_{\pm} = p_x \pm ip_y$, and $w_{\mathbf{p}}^{\mu} = [(\overline{v}^{\mu}p_x + w_H^{\mu})^2 + (\overline{v}^{\mu}p_y)^2]^{1/2}$. In the above equation $A_i(\xi_{\mathbf{p}}^{\mu\pm})$ and $B_i(\xi_{\mathbf{p}}^{\mu\pm})$ are the Airy functions with arguments

$$\xi_{\mathbf{p}}^{\mu\pm} = \frac{z}{l_{\perp}^{\mu}} + \frac{\varepsilon_{\mathbf{p}}^{\mu\pm} - E + \delta_b^{\mu}\Delta E_c}{\varepsilon_{\perp}^{\mu}}, \quad (3)$$

with δ_{μ}^{b} acting as a Kronecker function and $l_{\perp}^{\mu} = \left(\hbar^2/2m_{\mu}eF_{\perp}\right)^{1/3}$, $\varepsilon_{\perp}^{\mu} = \hbar^2/[2m_{\mu}\left(l_{\perp}^{\mu}\right)^2]$, and $\varepsilon_{\mathbf{p}}^{\mu\pm} = \varepsilon_p^{\mu} \pm |w_{\mathbf{p}}^{\mu}|$. Finally, $a_{\mu\pm}$, $b_{\mu\pm}$ are unknown coefficients that we will obtain by means of the boundary conditions, which include abrupt interface parameter $\chi = (2eF_{\perp}\delta + \Delta E_c)/2\varepsilon_g \approx \Delta E_c/2\varepsilon_g$, where δ is the halfwidth of that interface [4].

Now we generate transfer matrices, $M^{\mu}(L_i, E, \mathbf{p})$, which include boundary conditions at interface L_i. To obtain electronic levels for each 2D momentum $\mathbf{p} = (p_x, p_y)$ we introduce a modification of the method used before [3]. The total transfer matrix can be written as:

$$\begin{aligned} S(E,\mathbf{p}) &= [M^b(L_1,E,\mathbf{p})]^{-1} \cdot M^w(L_1,E,\mathbf{p}) \cdot [M^w(L_2,E,\mathbf{p})]^{-1} \cdot M^b(L_2,E,\mathbf{p}) \cdot \\ &\quad [M^b(L_3,E,\mathbf{p})]^{-1} \cdot M^w(L_3,E,\mathbf{p}) \cdot [M^w(L_4,E,\mathbf{p})]^{-1} \cdot M^b(L_4,E,\mathbf{p}). \end{aligned} \quad (4)$$

And the exact solution of the Hamiltonian is obtained from the Wronskyan-like:

$$S_w\left(E,\mathbf{p}\right)=S_{11}\left(E,\mathbf{p}\right)\cdot S_{33}\left(E,\mathbf{p}\right)-S_{31}\left(E,\mathbf{p}\right)\cdot S_{13}\left(E,\mathbf{p}\right)=0 \tag{5}$$

Fig. 2 represents $S_w\left(E,\mathbf{p}\right)$, $S_{11}\left(E,\mathbf{p}\right)$ and $S_{33}\left(E,\mathbf{p}\right)$ versus E for a given momentum $\mathbf{p}$. Solutions of Eq. (1) correspond to their roots: $S_w\left(E,\mathbf{p}\right)$ has four roots for each $\mathbf{p}$ value, corresponding to the two deepest coupled levels of the ACQW, and their respective spin down and spin up sublevels. In order to identify spin orientation, we look for $S_{11}\left(E,\mathbf{p}\right)$ roots, which correspond to the two coupled levels with spin up. On the other hand, $S_{33}\left(E,\mathbf{p}\right)$ roots indicate spin down sublevels. Sweeping over a wide range of values of $\mathbf{p}$ we obtain dispersion relations as four paraboloids.

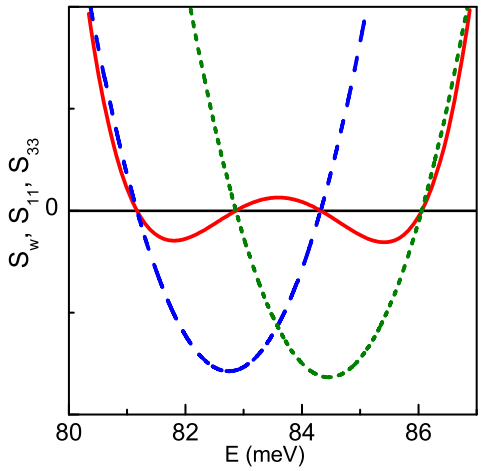

Figure 2. Solutions of the transcendental Eq. (5). $S_w\left(E,\mathbf{p}\right)$: red solid line. Spin down solutions $S_{33}\left(E,\mathbf{p}\right)$: blue dashed line. Spin up solutions $S_{11}\left(E,\mathbf{p}\right)$: green dotted line.

Once energy and coefficients $a_{\mu\sigma}$, $b_{\mu\sigma}$ (Eq. 2) have been obtained, we normalize wave functions for each momentum $\mathbf{p}$. Scheme of Fig. 1 includes the two resonant energy levels and the respective wave functions for $\mathbf{p}=\mathbf{0}$. Spin levels are indistinguishable in this figure.

3. Results

We present here numerical results for $In_{0.53}Ga_{0.47}As-In_{0.52}Al_{0.48}As$-based ACQWs [5] and formed by two $InGaAs$ wells of 50 and 100 Å wide separated by a 40 Å $InAlAs$ barrier. We have applied an electric field of 67 kV/cm to get resonance of the deepest conduction levels. We have used a magnetic field of 0.5 T. We can find for this field an anticrossing between sublevels spin down and up at each electronic level.

The four paraboloids corresponding to the two lower electronic levels after spin splitting are represented in Fig. 3, where spin anticrossing is visible at the right of the two sets of paraboloids. Spin anticrossing occurs around $p_x/p_0=30$ for $p_y/p_0=0$, where $p_0=m_w\overline{v}^w$. Note that paraboloids have not rotation symmetry because the magnetic energy $w^{\mu}_{\mathbf{p}}$, which is an essential part of the Airy functions argument, induces a breaking of the p_x momentum symmetry and, as a consequence, the spin anticrossing.

In Fig. 4 we present a $p_y=0$ section of the former figure where we can get a more accurate 2D description of the anticrossing p_x position and energy splitting.

Interestingly, interface contributions are opposite to the intrinsic spin-orbit effect. The mechanisms contributing to mix Pauli contribution with the other kinds of spin-orbit contributions (low magnetic field or interface effects) are different. As a consequence, numerical

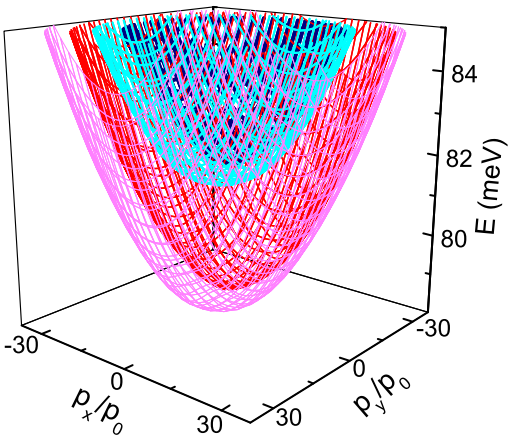

Figure 3. Energy versus p_x and p_y. From bottom to top: first level, spin down and spin up, second level, spin down and spin up.

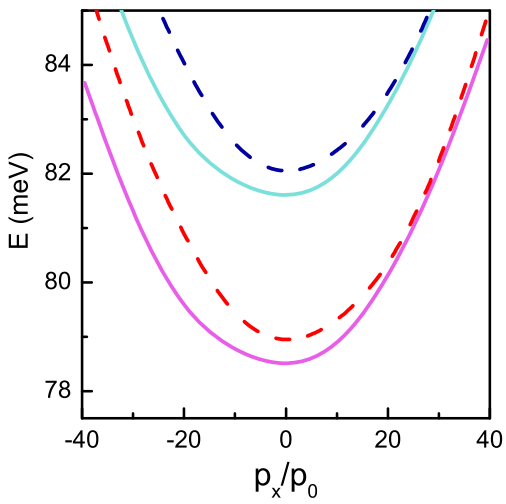

Figure 4. Energy versus p_x for $p_y = 0$. Solid line: spin down, dashed line: spin up.

calculations for $InGaAs - InAlAs$ structures, subjected to very low in-plane magnetic fields, lead to pronounced magnetoinduced changes in the energy dispersion relations, This effect is particularly noticeable for spin anticrossings.

4. Conclusions

In this work we have presented an improved modification of the transfer matrix approximation. So we have raised 4×4 matrices to include spin sublevels from the Pauli (Zeeman) splitting caused by a magnetic field and the effect of abrupt interfaces. Although we have limited ourselves to include these two contributions, the method is capable of handling any other contribution to the spin splitting. We have applied the method to narrow-gap ACQWs under transverse electric and in-plane magnetic fields. We have used non-symmetric contour conditions, caused by the asymmetry of the structure, to solve the eigenvalue problem. The present version of the transfer matrix, based on the Wronskian-like of wave functions space, has proven to be a highly efficient and effective tool to study the physical properties of any layered material when subjected to a wide range of perturbations. In particular, the method is especially useful in analyzing spin peculiarities.

References

[1] Bernevig B A and Zhang S 2006 *IBM J. Res. and Dev.***50** 1. Kikkawa J M and Awschalom D D 1998 *Phys. Rev. Lett.*. **80** 4313
[2] Hernández-Cabrera A, Aceituno P and Vasko F T 2008 *Journal of Luminescence* **128** 862. Hernández-Cabrera A, Aceituno P and Vasko F T 2006 *Phys. Rev.* B **74** 035330
[3] Hernández-Cabrera A and Aceituno P 2014 *Indian J. Phys* In press.
[4] Vasko F T and Kuznetsov A V 1999 *Electronic States and Optical Transitions in Semiconductor Heterostructures* (New York: Springer)
[5] Vurgaftman I, Meyer J R and Ram-Mohan L R 2001 *J. Appl. Phys* **89** 5815